Pergamon

Int. J. Solids Structures Vol. 33, No. 19, pp. 2789–2815, 1996

0020-7683/96 $15.00 + .00

0020-7683(95)00179-4

SCATTERING OF ELASTIC WAVES BY A RIGID CYLINDRICAL INCLUSION PARTIALLY DEBONDED FROM ITS SURROUNDING MATRIX—I. SH CASE

YUE-SHENG WANG† and DUO WANG
Department of Astronautics and Mechanics, P.O. Box 344, Harbin Institute of Technology, Harbin 150001, P.R. China

(*Received* 18 *April* 1994; *in revised form* 26 *May* 1995)

Abstract—In Part I of this two-part paper, the scattering of SH waves by a rigid cylindrical inclusion partially debonded from its surrounding matrix is investigated by using the wave function expansion method and singular integral equation technique. The debonding regions are modeled as multiple arc-shaped interface cracks with non-contacting faces. Expressing the scattered fields as the wave function expansions with unknown coefficients and considering the mixed boundary conditions, we reduce the problem to a set of simultaneous dual series equations. Then dislocation density functions are introduced as unknowns to transform these dual series equations to a set of singular integral equations of the first type which can be easily solved numerically by using the quadrature method of Erdogan and Gupta [*Int. J. Solids Structures* **7**, 1089–1107 (1972)]. The solution is valid for arbitrary values of $K_{T0}r_0$ (where K_{T0} is the wave number and r_0 the inclusion radius) and arbitrary numbers and sizes of the debonds. Explicit solutions are obtained in two limiting situations: (i) the long wavelength limit ($K_{T0}r_0 \ll 1$). In this case, the solution reduces to the quasistatic solution; (ii) the small debond limit with $K_{T0}r_0 = O(1)$. This means the wavelength greatly exceeds the debond size and the solution is identical to that of a flat interface crack between a rigid half space and an elastic one subjected to static loading at infinity. If the debond is small and $K_{T0}r_0 \gg 1$, the solution will give the results of a flat interface crack subjected to an incident SH wave. Finally, the numerical results of the dynamic stress intensity factors, the rigid body translations of the inclusion and the scattering cross-sections are presented for an inclusion with one or two debonds. The phenomenon of low frequency resonance discovered by Yang and Norris [*J. Mech. Phys. Solids* **39**, 273–294 (1991)] for an elastic inclusion with one debond is shown and its dependence upon the various parameters is discussed. The solution of this problem is relevant to ultrasonic nondestructive detection of debonding and is expected to have applications to the question of how dynamic loading can lead to growth of debonds [Norris and Yang, *Mech. Mater.* **11**, 163–175 (1991)]. Copyright © 1996 Elsevier Science Ltd.

1. INTRODUCTION

The scattering of elastic waves by inclusion in an elastic medium has been a topic of interest to many researchers because of its practical importance in earthquake engineering, nondestructive evaluation, etc. In most published literature, the inclusion was assumed to be perfectly bonded with the matrix, i.e. the interface is completely welded so that the tractions and displacements are continuous across the interface. However, this is not always true in practical cases. Partial debonding usually occurs at the interface, which may result in catastrophic failure of structures. The nondestructive detection of debonding and the forecast of possible growth of debonds under dynamic loading are of importance to engineers. Thus, the dynamic analysis of a partially debonded inclusion subjected to elastic waves received considerable attention in recent years.

Parton and Kudryavtsev (1975) first attacked the problem of interaction of SH waves with a fixed rigid cylindrical inclusion with one debond at the interface. They treated the debond as an interface crack and obtained the dynamic stress intensity factor. The method they used is very complicated and no more problems have been solved by this method since then, except Belyaev (1985) who considered a hollow elastic cylindrical inclusion. Coussy (1982, 1983) dealt with the problems of SH wave and P wave scattering from an elastic

† Present address: Institute of Engineering Mechanics, Northern Jiaotong University, Beijing 100044, P.R. China.

cylindrical inclusion with an interface crack by the use of a perturbation method. She obtained closed form far-field solutions (i.e. the scattering cross-sections) which are valid only in the long wavelength limit. Recently, the same problem (SH wave incidence) was solved by Yang and Norris (1991) by reducing the problem to an integral equation in the crack opening displacement (COD) of the debond. The numerical results of the dynamic stress intensity factors and the scattering cross-sections exhibit a phenomenon of low frequency resonance which was not predicted by the quasistatic theory (Coussy, 1982, 1983). Later, they reconsidered the same problem by formulating the problem in terms of the unknown stress along the bonding region (Norris and Yang, 1991b). An asymptotic solution for a very large debond was derived, which successfully explains the low frequency resonance. This approach was also applied to the problem of the incident P wave by ignoring the oscillatory behavior of the stresses near the crack tips (Yang and Norris, 1992). Indeed, it is very difficult to deal with the problem including such oscillatory behavior by using this method.

It is worthwhile mentioning that some other methods have also been used to solve similar problems. Kitahara *et al.* (1989) considered the scattering problem from a spherical inclusion by boundary element method (BEM). In their work the interface is modeled as a distribution of springs and the case of a partial debonding is included by setting the spring constants to zero over the debonding region. Zhong and Lin (1992) applied the BEM to the scattering problem for anisotropic medium and considered the scattering of elastic waves by a partially debonded inclusion as a special example. The BEM is a powerful technique but cannot go to very high frequencies in practice. The null field approach has been used by Boström and Olsson (1987) and Olsson and Boström (1989) to study the scattering problems of non-planar cracks which may be viewed as a special case of interface cracks when the inclusion and matrix are made of the same material.

In this series of papers, we reconsider the scattering problem from a partially debonded inclusion by a different approach. The analysis is limited to a rigid inclusion but allows for multiple debonding regions which are modeled as multiple interface cracks with non-contacting faces. We reduce the problem to a set of dual series equations which is then converted to a set of singular integral equations in terms of the dislocation density functions. The singular integral equation technique has many advantages in solving the crack problems, especially the interface crack problems, since the derived singular integral equation describes the stress singularity of crack tips directly and its solution (analytical or numerical) is fully developed. In fact, this technique has been widely and successfully used in both static and dynamic flat interface crack problems [e.g. Erdogan and Gupta (1971), Yang and Bogy (1985)]. In Part I of this two-part paper we apply this approach to the scattering of SH waves. We not only obtain the numerical results but also derive the explicit solutions in two limiting cases: the long wavelength limit and the small debond limit. These results agree very well with those of Yang and Norris (1991) and Norris and Yang (1991b) when only one debond exists at the interface. Therefore the present method is proved to be successful and will be extended to the scattering of P and SV waves in Part II, where the oscillatory behavior we have mentioned before will be taken into account.

2. DESCRIPTION OF THE PROBLEM

Consider the problem shown in Fig. 1. A rigid cylindrical inclusion with radius r_0 and mass density ρ_1 is partially debonded from its surrounding elastic matrix. The debonds are modeled as n interface cracks. Use cylindrical coordinates (r, θ, z) $(-\pi \leqslant \theta \leqslant \pi)$, and let the θ coordinates of the kth crack tips be a_k and b_k $(k = 1\text{–}n)$. All motion is time harmonic with frequency ω, and the term $e^{-i\omega t}$ will be omitted for simplicity.

The incident SH wave propagates in the θ_0-direction with the form

$$w_0^{(i)}(r, \theta) = A\, e^{iK_{T0} r \cos(\theta - \theta_0)} \tag{1}$$

where $K_{T0} = \omega/C_{T0}$ is the wavenumber, $C_{T0} = \sqrt{\mu_0/\rho_0}$ is the shear wave velocity, μ_0 and ρ_0

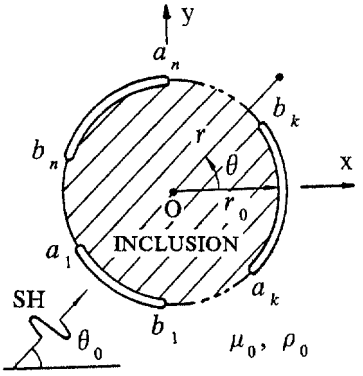

Fig. 1. A SH wave incident on a rigid cylindrical inclusion partially debonded from elastic matrix.

are, respectively, shear modulus and mass density of the matrix and A is amplitude. The total out-of-plane displacement in the matrix may be decomposed as

$$w_0(r,\theta) = w_0^{(i)}(r,\theta) + w_0^{(0)}(r,\theta) + w_0^{(1)}(r,\theta) \tag{2}$$

where $w_0^{(0)}$ is the scattered field that would be present if the inclusion were perfectly bonded (Pao and Mow, 1973), while $w_0^{(1)}$ is the additional scattered field generated by the debonds, which satisfies the following Helmholtz equation (Pao and Mow, 1973)

$$\nabla^2 w_0^{(1)} + K_{T0}^2 w_0^{(1)} = 0 \tag{3}$$

where

$$\nabla^2 = \frac{\partial^2}{\partial r^2} + \frac{1}{r}\frac{\partial}{\partial r} + \frac{1}{r^2}\frac{\partial^2}{\partial \theta^2}.$$

By the use of the wave function expansion method (Pao and Mow, 1972), $w_0^{(1)}$ can be written as

$$w_0^{(1)}(r,\theta) = \sum_{m=-\infty}^{\infty} A_m H_m^{(1)}(K_{T0}r)\,\mathrm{e}^{-\mathrm{i}m\theta} \tag{4}$$

where $H_m^{(1)}(\ )$ are the Hankel functions of the first kind, and A_m are unknown coefficients. The corresponding stress component $\tau_{rz0}^{(1)}$ is

$$\tau_{rz0}^{(1)}(r,\theta) = \mu_0 \frac{\partial w_0^{(1)}}{\partial r} = \mu_0 K_{T0} \sum_{m=-\infty}^{\infty} A_m H_m^{(1)'}(K_{T0}r)\,\mathrm{e}^{-\mathrm{i}m\theta} \tag{5}$$

For a movable rigid inclusion, we should also consider the motion of the inclusion. Under the action of SH waves, the inclusion will translate as a rigid body with its harmonic anti-plane motion $W_1\,\mathrm{e}^{-\mathrm{i}\omega t}$. Decompose W_1 as

$$W_1 = W_1^{(0)} + W_1^{(1)} \tag{6}$$

where $W_1^{(0)}$ is the amplitude of the rigid body translation of a perfectly bonded inclusion (Pao and Mow, 1973), and $W_1^{(1)}$ the amplitude of the additional translation due to debonding, which is governed by following kinetic equation

$$-\pi r_0^2 \omega^2 \rho_1 W_1^{(1)} = \int_{-\pi}^{\pi} r_0 \tau_{rz0}^{(1)}(r_0, \theta)\, \mathrm{d}\theta. \tag{7}$$

Substituting eqn (5) into eqn (7) yields

$$W_1^{(1)} = -2\rho \frac{H_0^{(1)'}(K_{T0} r_0)}{K_{T0} r_0} A_0 \tag{8}$$

where $\rho = \rho_0/\rho_1$ and A_0 is unknown.

The interface condition for the displacements may be written as

$$w_0^{(1)}(r_0, \theta) = \Delta w(\theta) \tag{9}$$

for a fixed rigid inclusion, or

$$w_0^{(1)}(r_0, \theta) - W_1^{(1)} = \Delta w(\theta) \tag{10}$$

for a movable rigid inclusion. Δw in eqns (9) and (10) is the discontinuity of the displacement across the interface, which can be expressed as

$$\Delta w(\theta) = \begin{cases} 0 & \theta \notin (a_k, b_k) \\ \Delta w_k(\theta) & \theta \in (a_k, b_k) \end{cases}, \quad k = 1\text{–}n \tag{11}$$

with Δw_k denoting the COD of the kth crack.

The total stress vanishes on the crack faces, that is

$$\tau_{rz0}^{(1)}(r_0, \theta) = -\tau(\theta), \quad \theta \in (a_k, b_k) \tag{12}$$

where we have denoted $\tau(\theta) = \tau_{rz0}^{(i)}(r_0, \theta) + \tau_{rz0}^{(0)}(r_0, \theta)$ which can be found in Pao and Mow (1973).

So far we have reduced the problem to finding the solutions of $w_0^{(1)}$ and $W_1^{(1)}$ or $A_m (m = -\infty\text{–}+\infty)$ satisfying the mixed boundary conditions (9)–(12).

3. DERIVATION AND SOLUTION OF THE SINGULAR INTEGRAL EQUATIONS

Expanding $\Delta w(\theta)$ defined by eqn (11) in a series of $\mathrm{e}^{-\mathrm{i}m\theta}$

$$\Delta w(\theta) = \sum_{m=-\infty}^{\infty} \Delta \bar{w}_m \mathrm{e}^{-\mathrm{i}m\theta} \tag{13}$$

where

$$\Delta \bar{w}_m = \frac{1}{2\pi} \int_{-\pi}^{\pi} \Delta w(\zeta) \mathrm{e}^{\mathrm{i}m\zeta}\, \mathrm{d}\zeta = \frac{1}{2\pi} \sum_{l=1}^{n} \int_{a_l}^{b_l} \Delta w_l(\zeta) \mathrm{e}^{\mathrm{i}m\zeta}\, \mathrm{d}\zeta, \tag{14}$$

we have

$$A_m = \frac{\Delta \bar{w}_m}{H_m^{(1)}(K_{T0} r_0)} \tag{15}$$

from eqns (4) and (9) for a fixed rigid inclusion or

$$A_m = \frac{\Delta\bar{w}_m}{H_m^{(1)}(K_{T0}r_0) + 2\rho \dfrac{H_0^{(1)'}(K_{T0}r_0)}{K_{T0}r_0}\delta_{0m}} \tag{16}$$

from eqns (4), (8) and (10) for a movable rigid inclusion. In eqn (16), δ_{0m} is Kronecker delta. Comparing eqn (15) with eqn (16), we can see that when $\rho = 0$, eqn (14) reduces to eqn (15). Thus the following analysis will be focused on a movable rigid inclusion and the results for a fixed rigid inclusion can be obtained by setting $\rho = 0$.

Substituting eqn (5) into eqn (12) and considering eqn (16), we have

$$\mu_0 K_{T0} \sum_{m=-\infty}^{\infty} N(m)\Delta\bar{w}_m \, e^{-im\theta} = -\tau(\theta), \quad \theta \in (a_k, b_k) \tag{17}$$

with

$$N(m) = H_m^{(1)'}(K_{T0}r_0)\left[H_m^{(1)}(K_{T0}r_0) + 2\rho \frac{H_0^{(1)'}(K_{T0}r_0)}{K_{T0}r_0}\delta_{0m}\right]^{-1}. \tag{18}$$

On the bonding regions, $\Delta w(\theta) = 0$, which implies

$$\sum_{m=-\infty}^{\infty} \Delta\bar{w}_m \, e^{-im\theta} = 0, \quad \theta \notin (a_k, b_k) \tag{19}$$

Equations (17) and (19) are dual series equations of the problem. If we substitute eqn (14) into eqn (17), we will have a set of integral equations in terms of the COD as Yang and Norris (1991) derived for the case of an elastic inclusion with one debond. Here, instead of doing so, we will transform eqns (17) and (19) to a set of singular integral equations. To this end, we introduce the dislocation density function of the kth crack

$$\varphi_k(\theta) = \frac{1}{r_0}\frac{\partial}{\partial\theta}(\Delta w_k), \quad k = 1\text{–}n \tag{20}$$

and denote

$$\varphi(\theta) = \begin{cases} 0 & \theta \notin (a_k, b_k) \\ \varphi_k(\theta) & \theta \in (a_k, b_k) \end{cases}, \quad k = 1\text{–}n. \tag{21}$$

It can then be shown that $\Delta w(\theta)$ may be expressed as

$$\Delta w(\theta) = r_0 \int_{-\pi}^{\theta} \varphi(\zeta)\, d\zeta \tag{22}$$

which when substituted into eqn (14) yields

$$\Delta\bar{w}_0 = \frac{r_0}{2\pi}\int_{-\pi}^{\pi}\left[\int_{-\pi}^{\theta}\varphi(\zeta)\, d\zeta\right]d\theta = -\frac{r_0}{2\pi}\sum_{l=1}^{n}\int_{a_l}^{b_l}\left(\theta - \frac{a_l+b_l}{2}\right)\varphi_l(\theta)\, d\theta \tag{23a}$$

$$\Delta\bar{w}_m = \frac{r_0}{2\pi}\int_{-\pi}^{\pi}\left[\int_{-\pi}^{\theta}\varphi(\zeta)\, e^{im\zeta}\, d\zeta\right]d\theta = \frac{i}{2\pi}\frac{r_0}{m}\sum_{l=1}^{n}\int_{a_l}^{b_l}\varphi_l(\theta)\, e^{im\theta}\, d\theta \tag{23b}$$

where we have used by-part integration. The reason for the appearance of $(a_l+b_l)/2$ in eqn (23a) is that when $\varphi_l(\theta)$ is symmetric about $\theta = (a_l+b_l)/2$, $\Delta\bar{w}_0 = 0$. Substituting eqns (23a,b) into eqn (17), we obtain the integral equations

$$\frac{\mathrm{i}}{2\pi}\sum_{l=1}^{n}\int_{a_l}^{b_l}\sum_{m=-\infty}^{\infty}M(m)\varphi_l(\zeta)\,\mathrm{e}^{\mathrm{i}m(\zeta-\theta)}\,\mathrm{d}\zeta=-\tau(\theta),\quad \theta\in(a_k,b_k) \tag{24}$$

where

$$M(0)=\mathrm{i}\mu_0 K_{T0} r_0 N(0)\left(\zeta-\frac{a_l+b_l}{2}\right),\quad M(m)=\mu_0 K_{T0} r_0 m^{-1}N(m),\quad m\neq 0. \tag{25a,b}$$

The Hankel functions $H_m^{(1)}(z)$ have following useful properties (Abramowitz and Stegun, 1965)

$$H_m^{(1)}(z)\to-\frac{(m-1)!}{\pi}\left(\frac{2}{z}\right)^m\mathrm{i},\quad m\to+\infty \tag{26a}$$

$$H_{-m}^{(1)}(z)=(-1)^m H_m^{(1)}(z). \tag{26b}$$

Therefore, we have

$$M(m)\approx-\mathrm{sgn}(m)\mu_0+O(m^{-2}),\quad m\to\pm\infty. \tag{27}$$

Assuming

$$P(\zeta,\theta)=\frac{\mathrm{i}}{2\pi}\left\{M(0)+2\mathrm{i}\sum_{m=1}^{\infty}[M(m)+\mu_0]\sin m(\zeta-\theta)\right\} \tag{28}$$

and using the following relation

$$\sum_{|m|=1}^{\infty}\mathrm{sgn}(m)\,\mathrm{e}^{\mathrm{i}m(\zeta-\theta)}=\mathrm{i}\cot\left(\frac{\zeta-\theta}{2}\right), \tag{29}$$

we can transform eqn (24) into a set of Hilbert singular integral equations of the first type

$$\frac{\mu_0}{2\pi}\sum_{l=1}^{n}\int_{a_l}^{b_l}\varphi_l(\zeta)\cot\left(\frac{\zeta-\theta}{2}\right)\mathrm{d}\zeta+\sum_{l=1}^{n}\int_{a_l}^{b_l}\varphi_l(\zeta)P(\zeta,\theta)\,\mathrm{d}\zeta=-\tau(\theta),\quad \theta\in(a_k b_k) \tag{30}$$

where $\varphi_k(\theta)$ should also satisfy the single-valued condition

$$\int_{a_k}^{b_k}\varphi_k(\zeta)\,\mathrm{d}\zeta=0. \tag{31}$$

By the use of the following substitutions

$$\begin{cases}\theta=c_k\xi+d_k,\quad \zeta=c_l\eta+d_l\\ \Phi_l(\eta)=\varphi_l(c_l\eta+d_l)\\ L(\eta,\xi)=\dfrac{1}{\mu_0}P(c_l\eta+d_l,c_k\xi+d_k)+\dfrac{1}{2\pi}\cot\left(\dfrac{c_l\eta-c_k\xi+d_l-d_k}{2}\right)-\dfrac{\delta_{kl}}{\pi c_k(\eta-\xi)}\end{cases} \tag{32}$$

where $c_k=(b_k-a_k)/2$ and $d_k=(b_k+a_k)/2$, eqn (30) can be further converted to a set of standard Cauchy singular integral equations

$$\frac{1}{\pi}\int_{-1}^{1}\frac{\Phi_k(\eta)}{\eta-\xi}\,d\eta+\sum_{l=1}^{n}\int_{-1}^{1}c_l\Phi_l(\eta)L(\eta,\xi)\,d\eta=-\frac{1}{\mu_0}\tau(c_k\xi+d_k),\quad|\xi|<1 \tag{33}$$

and eqn (31) becomes

$$\int_{-1}^{1}\Phi_k(\eta)\,d\eta=0. \tag{34}$$

In eqn (33), $L(\eta, \xi)$ is a Fredhelm integral kernel without any singularity. According to the general theory of singular integral equations (Muskhelishvili, 1953), we immediately know that $\Phi_k(\eta)$ has inverse square root behavior at $\eta = \pm 1$. Thus, setting

$$\Phi_k(\eta)=\frac{F_k(\eta)}{\sqrt{1-\eta^2}} \tag{35}$$

and applying the quadrature method developed by Erdogan and Gupta (1972), we obtain a set of linear algebraic equations from eqns (33) and (34)

$$\begin{cases}\dfrac{1}{N}\displaystyle\sum_{j=1}^{N}\sum_{l=1}^{n}\left[\frac{1}{\eta_j-\xi_i}+\pi c_l L(\eta_j,\xi_i)\right]F_l(\eta_j)=-\frac{1}{\mu_0}\tau(c_k\xi_i+d_k)\\[2ex]\dfrac{\pi}{N}\displaystyle\sum_{j=1}^{N}F_k(\eta_j)=0\end{cases} \tag{36}$$

where $\eta_j=\cos(\pi/2N)(2j-1)$, $\xi_i=\cos\pi i/N$, $i=1\text{–}N-1$, $k=1\text{–}n$, and N is the number of the discrete points of $F_k(\eta)$ between -1 and $+1$.

4. DYNAMIC STRESS INTENSITY FACTORS AND RIGID BODY MOTION OF THE INCLUSION

The dynamic stress intensity factors (DSIFs) at the kth crack tips a_k and b_k are defined as

$$K_{\mathrm{III}b_k}=\lim_{\theta\to b_k^{+}}[\sqrt{2r_0(\theta-b_k)}\tau_{rz}(r_0,\theta)] \tag{37a}$$

$$K_{\mathrm{III}a_k}=\lim_{\theta\to a_k}[\sqrt{2r_0(a_k-\theta)}\tau_{rz}(r_0,\theta)] \tag{37b}$$

where $\tau_{rz}(r_0,\theta)=\tau_{rz0}^{(i)}(r_0,\theta)+\tau_{rz0}^{(0)}(r_0,\theta)+\tau_{rz0}^{(1)}(r_0,\theta)$ and $\tau_{rz0}^{(1)}$ is

$$\tau_{rz0}^{(1)}(r_0,\theta)=\frac{\mu_0}{2\pi}\sum_{l=1}^{n}\int_{a_l}^{b_l}\varphi_l(\zeta)\cot\left(\frac{\zeta-\theta}{2}\right)d\zeta+\sum_{l=1}^{n}\int_{a_l}^{b_l}\varphi_l(\zeta)P(\zeta,\theta)\,d\zeta,\quad\theta\notin(a_k,b_k). \tag{38}$$

By considering eqn (32), the principal part of $\tau_{rz}(r_0, \theta)$ as $\theta\to a_k^{-}$ and b_k^{-} [or $\tau_{rz}(r_0, c_k\xi+d_k)$ as $\xi\to -1^{-}$ and 1^{+}] can easily be written as

$$\tau_{rz}(r_0,\theta)=\tau_{rz}(r_0,c_k\xi+d_k)\approx\frac{\mu_0}{\pi}\int_{-1}^{1}\frac{\Phi_k(\eta)}{\eta-\xi}\,d\eta. \tag{39}$$

Representing $F_k(\eta)$ in eqn (35) by a series in Chebyshev polynomials $T_j(\eta)$

$$F_k(\eta) = \sum_{j=0}^{\infty} A_j^{(k)} T_j(\eta) \tag{40}$$

and substituting it into eqn (39) yields

$$K_{\mathrm{III}b_k} = \mu_0\sqrt{r_0 c_k}F_k(1), \quad K_{\mathrm{III}a_k} = \mu_0\sqrt{r_0 c_k}F_k(-1) \tag{41a,b}$$

where we have used the relation

$$\frac{1}{\pi}\int_{-1}^{1} \frac{(1-\eta^2)^{-1/2}T_j(\eta)}{\eta-\xi}\,\mathrm{d}\eta = \frac{[(\xi^2-1)^{1/2}-\xi]^j}{(-1)^{j+1}(\xi^2-1)^{1/2}}, \quad |\xi| > 1. \tag{42}$$

The amplitude of the total rigid body translation (RBT) of the inclusion may be expressed, from eqns (6), (8) and (16), as

$$W_1 = W_1^{(0)} + W_1^{(1)} = W_1^{(0)} - \frac{2\rho H_0^{(1)'}(K_{T0}r_0)\Delta\bar{w}_0}{K_{T0}r_0 H_0^{(1)}(K_{T0}r_0) + 2\rho H_0^{(1)'}(K_{T0}r_0)} \tag{43}$$

where $W_1^{(0)}$ may be found in Pao and Mow (1973), and $\Delta\bar{w}_0$ may be derived, by the use of eqns (23a), (32), (35) and Gauss–Chebyshev integration formula (Abramowitz and Stegun, 1965), as

$$\Delta\bar{w}_0 = -\frac{r_0}{2}\sum_{l=1}^{n}\left[\frac{c_l^2}{N}\sum_{j=1}^{N}\eta_j F_l(\eta_j)\right]. \tag{44}$$

5. SCATTERED FAR-FIELD PATTERN AND SCATTERING CROSS-SECTION

Using the asymptotic expansions of Hankel functions in the far field (Abramowitz and Stegun, 1965), we may derive the following asymptotic expressions for the scattered far-field displacement

$$w_0^{(0)}(r,\theta) + w_0^{(1)}(r,\theta) \approx \sqrt{\frac{8\pi}{K_{T0}r}}\,\mathrm{e}^{\mathrm{i}\left(K_{T0}r-\frac{\pi}{4}\right)}F(\theta,\theta_0), \quad r\to\infty \tag{45}$$

where $F(\theta,\theta_0) = F^{(0)}(\theta,\theta_0) + F^{(1)}(\theta,\theta_0)$, $F^{(0)}(\theta,\theta_0)$ is the scattered far-field pattern for a perfectly bonded inclusion, which can be calculated from the results of Pao and Mow (1973), and $F^{(1)}(\theta,\theta_0)$ is that due to debonding, which follows from eqns (4), (16), (23a,b), (32), (35) and Gauss–Chebyshev integration formula as

$$F^{(1)}(\theta,\theta_0) = -\frac{r_0}{4\pi}\frac{K_{T0}r_0}{K_{T0}r_0 H_0^{(1)}(K_{T0}r_0) + 2\rho H_0^{(1)'}(K_{T0}r_0)}\sum_{l=1}^{n}\left[\frac{c_l^2}{N}\sum_{j=1}^{N}\eta_j F_l(\eta_j)\right]$$
$$-\sum_{m=1}^{\infty}\left\{\frac{r_0}{2\pi}\frac{\mathrm{i}^{-m}}{mH_m^{(1)}(K_{T0}r_0)}\sum_{l=1}^{n}\left[\frac{c_l}{N}\sum_{j=1}^{N}F_l(\eta_j)\sin m(c_l\eta_j + d_l - \theta)\right]\right\}. \tag{46}$$

The total energy flux for the scattered field is the time average of the flux over any surface S enclosing the inclusion (Pao and Mow, 1973)

$$\langle P^s\rangle = \frac{\omega}{2}\,\mathrm{Im}\int_S (w_0^{(0)} + w_0^{(1)})^* \cdot (\tau_{rz0}^{(0)} + \tau_{rz0}^{(1)})\,\mathrm{d}s \tag{47}$$

where asterisk represents conjugation. Choosing S as a unit-length cylindrical surface with

radius of infinitely large and using the expression of scattered far-field displacement given by eqn (45), we have

$$\langle P^s \rangle = 4\pi\omega\mu_0 \int_{-\pi}^{\pi} |F(\theta, \theta_0)|^2 \, \mathrm{d}\theta. \tag{48}$$

The total scattering cross-section (SCS) is defined as (Pao and Mow, 1973)

$$\sigma(\omega) = \frac{\langle P^s \rangle}{\langle \dot{e}_0 \rangle} \tag{49}$$

where

$$\langle \dot{e}_0 \rangle = \frac{\omega}{2} \operatorname{Im} [(w_0^{(i)})^* \cdot \tau_{r=0}^{(i)}] = \frac{\omega}{2} \mu_0 K_{T0} |A|^2 \tag{50}$$

is the time average of the incident flux.

In addition, following the two-dimensional optical theorem, $\sigma(\omega)$ may be expressed as

$$\sigma(\omega) = -\frac{8\pi}{K_{T0}|A|^2} \operatorname{Re} [A^* \cdot F(\theta_0, \theta_0)] \tag{51}$$

which may be used as a check on the numerical computations.

6. THE LONG WAVELENGTH LIMIT

The long wavelength limit is also called the quasistatic limit, that is, the quasistatic solution may be recovered from the dynamic solution as the incident wavelength greatly exceeds the inclusion radius, i.e. $K_{T0} r_0 \ll 1$. In this limiting case, by considering the properties of Bessel functions with small argument (Abromowitz and Stegun, 1965), we may note that $M(m)$ of eqns (25a,b) become

$$M(0) = O(K_{T0} r_0); \quad M(m) = -\operatorname{sgn}(m)\mu_0 + O(K_{T0} r_0), \quad m \neq 0 \tag{52a,b}$$

and therefore

$$\sum_{m=-\infty}^{\infty} M(m) \, \mathrm{e}^{\mathrm{i}m(\zeta-\theta)} = -\mathrm{i}\mu_0 \cot\left(\frac{\zeta-\theta}{2}\right) + O(K_{T0} r_0). \tag{53}$$

Similarly, $\tau(\theta)$ in eqn (24) becomes

$$\tau(\theta) = 2\tau_0 [\cos(\theta - \theta_0) + o(1)] \tag{54}$$

with $\tau_0 = \mathrm{i}\mu_0 A K_{T0}$. Then eqn (24) reduces to a Hilbert singular integral equation of the form

$$\frac{\mu_0}{2\pi\mathrm{i}} \sum_{l=1}^{n} \int_{a_l}^{b_l} \varphi_l(\zeta) \cot\left(\frac{\zeta-\theta}{2}\right) \mathrm{d}\zeta = 2\mathrm{i}\tau_0 \cos(\theta - \theta_0), \quad \theta \in (a_k, b_k) \tag{55}$$

of which the solution satisfying eqn (21) and $\varphi_k(\pm\infty\mathrm{i}) = 0$ is (Lu, 1965)

$$\varphi_k(\theta) = \frac{i\tau_0}{\mu_0}\frac{X(\theta)}{\pi i}\sum_{l=1}^{n}\int_{a_l}^{b_l}\cos(\zeta-\theta_0)X^{-1}(\zeta)\left[\cot\left(\frac{\zeta-\theta}{2}\right)-\tan\frac{\theta}{2}\right]d\zeta \tag{56}$$

where

$$X(z) = \prod_{l=1}^{n}\left(\tan\frac{z}{2}-\tan\frac{a_l}{2}\right)^{-1/2}\left(\tan\frac{z}{2}-\tan\frac{b_l}{2}\right)^{-1/2}, \quad \lim_{z\to\pm\pi}\tan\frac{z}{2}X(z) = 1, \quad X(\theta) = X^{+}(\theta). \tag{57}$$

In the following analysis we will only consider the case of one debond, i.e. $n = 1$. Set $b_1 = -a_1 = \alpha$, then eqn (56) becomes

$$\varphi_1(\theta) = \frac{i\tau_0}{\mu_0}\frac{X(\theta)}{\pi i}\int_{-\alpha}^{\alpha}\cos(\zeta-\theta_0)X^{-1}(\zeta)\left[\cot\left(\frac{\zeta-\theta}{2}\right)-\tan\frac{\theta}{2}\right]d\zeta \tag{58}$$

where

$$\begin{aligned} X(\theta) &= \left(\tan^2\frac{\theta}{2}-\tan^2\frac{\alpha}{2}\right)^{-1/2}, \quad |\theta| > \alpha \\ &= -i\left(\tan^2\frac{\alpha}{2}-\tan^2\frac{\theta}{2}\right)^{-1/2}, \quad |\theta| < \alpha. \end{aligned} \tag{59}$$

The static stress intensity factors (SSIFs) are defined by analogy with eqns (37a,b). From the results of Section 4, we have, at the crack tip $\theta = +\alpha$

$$K_{III}^{+} = -i\mu_0\lim_{\theta\to\alpha^{+}}\sqrt{2r_0(\theta-\alpha)}\varphi_1(\theta). \tag{60}$$

Substitution of eqns (58)–(60) yields

$$K_{III}^{+} = -\frac{\tau_0}{\pi}\sqrt{2r_0}\sec\frac{\alpha}{2}\sqrt{\cot\frac{\alpha}{2}}\int_{-\alpha}^{\alpha}\cos(\zeta-\theta_0)\sqrt{\frac{\tan\frac{\alpha}{2}+\tan\frac{\zeta}{2}}{\tan\frac{\alpha}{2}-\tan\frac{\zeta}{2}}}d\zeta. \tag{61}$$

Evaluating the integral in the above equation (see Appendix A), we obtain

$$K_{III}^{+} = -2\tau_0\sqrt{r_0\sin\alpha}\cos\left(\theta_0-\frac{\alpha}{2}\right) \tag{62}$$

which is the same form as eqn (53) of Yang and Norris (1991) if we set $\mu_2 \to \infty$ in their equation. Therefore one may say that the DSIF in the long wavelength limit reduces to the SSIF for a uniform anti-plane stress τ_0 at infinity which is inclined at the angle θ_0.

As $K_{T0}r_0 \to 0$, $W_1^{(0)}$ (Pao and Mow, 1973) behaves like

$$W_1^{(0)} = A[1+o(1)] \tag{63}$$

and $W_1^{(1)}$ follows from eqns (8), (16) (23a) and (58) as

$$W_1^{(1)} \approx -\Delta\bar{w}_0 = \frac{r_0}{2\pi}\int_{-\alpha}^{\alpha} \theta\varphi_1(\theta)\,\mathrm{d}\theta = A\cdot O(K_{T0}r_0) \tag{64}$$

which means that for very low frequency, the presence of the debond only produces a change of order $K_{T0}r_0$ in the RBT.

The scattered far-field pattern for a perfectly bonded rigid inclusion becomes, in the long wavelength limit,

$$F^{(0)}(\theta,\theta_0) = \frac{A\mathrm{i}}{8}(K_{T0}r_0)^2[\rho^{-1}-1-2\cos(\theta-\theta_0)]+o((K_{T0}r_0)^2). \tag{65}$$

The additional far-field pattern due to the debond follows from eqns (4), (16), (23a,b) and (58) as

$$\begin{aligned} F^{(1)}(\theta,\theta_0) &= -\frac{K_{T0}r_0^2}{4\pi}\int_{-\alpha}^{\alpha}\varphi_1(\eta)\sin(\eta-\theta)\,\mathrm{d}\eta+o((K_{T0}r_0)^2) \\ &= -\frac{A\mathrm{i}}{4\pi^2}(K_{T0}r_0)^2\int_{-\alpha}^{\alpha}X(\eta)\sin(\eta-\theta)\int_{-\alpha}^{\alpha}\cos(\zeta-\theta_0)X^{-1}(\zeta) \\ &\quad\cdot\left[\cot\left(\frac{\zeta-\eta}{2}\right)-\tan\frac{\eta}{2}\right]\mathrm{d}\zeta\,\mathrm{d}\eta+o((K_{T0}r_0)^2). \end{aligned} \tag{66}$$

Evaluating the double integral (see Appendix B), we obtain

$$F^{(1)}(\theta,\theta_0) \sim \frac{A\mathrm{i}}{2}(K_{T0}r_0)^2\left[\left(1-\cos^4\frac{\alpha}{2}\right)\cos\theta\cos\theta_0+\sin^4\frac{\alpha}{2}\sin\theta\sin\theta_0\right]+o((K_{T0}r_0)^2). \tag{67}$$

Here, for a rigid inclusion we have reobtained the quasistatic solution of Coussy (1982) which was also discussed by Yang and Norris (1991) for an elastic inclusion. The SCS calculated from eqns (65) and (67) for very low frequency does not exhibit a resonance phenomenon as shown by Yang and Norris (1991).

7. THE SMALL DEBOND LIMIT

This limiting case has been considered by Yang and Norris (1991) for an elastic inclusion with one debond. But they limited their analysis to the case of $K_{T0}r_0 = O(1)$ or $K_{T0}r_0 \ll 1$, that is, the incident wavelength is comparable with or larger than the inclusion radius and thus greatly exceeds the debond size. In this section, we reconsider this limiting case by allowing for arbitrary values of incident wavelength. We also focus our attention on one debond and assume $b_1 = -a_1 = \alpha \ll 1$. Under the substitutions $\zeta = \alpha\eta$, $\theta = \alpha\xi$ and $\Phi_1(\eta) = \varphi_1(\alpha\eta)$, eqn (24) becomes

$$\frac{\mathrm{i}\alpha}{2\pi}\int_{-1}^{1}\Phi_1(\eta)\sum_{m=-\infty}^{\infty}\bar{M}(m)\,\mathrm{e}^{\mathrm{i}m\alpha(\eta-\xi)}\,\mathrm{d}\eta = -\tau(\alpha\xi), \quad |\xi|<1 \tag{68}$$

where $\bar{M}(0) = \mathrm{i}\alpha\mu_0K_{T0}r_0N(0)\eta$ and $\bar{M}(m) = \mu_0K_{T0}r_0m^{-1}N(m)$ with $N(m)$ given by eqn (25). Set $s = m\alpha$. Then we have

$$\sum_{m=-\infty}^{\infty} \bar{M}(m)\, e^{im\alpha(\eta-\xi)} \approx \int_{-\infty}^{\infty} \alpha^{-1} \bar{M}(s/\alpha)\, e^{is(\eta-\xi)}\, ds$$

$$= 2i \int_{0}^{\infty} \alpha^{-1} \bar{M}(s/\alpha) \sin[s(\eta-\xi)]\, ds \equiv I. \tag{69}$$

Following the Debye's asymptotic expressions of Bessel functions (Abramowitz and Stegun, 1965), we have

$$\frac{zH_v^{(1)'}(vz)}{H_v^{(1)}(vz)} \to \begin{cases} -\sqrt{1-z^2}, z<1 \\ i\sqrt{z^2-1}, z>1 \end{cases}, \quad v \to +\infty, \quad z>0 \tag{70}$$

If we set $v = s/\alpha$ and $z = K_{T0}b/s$ with $b = r_0\alpha \ll 1$, $\bar{M}(s/\alpha)$ may be evaluated as

$$\bar{M}(s/\alpha) \approx -\mu_0 \bar{\beta}(s)/s \tag{71}$$

where

$$\bar{\beta}(s) = \sqrt{s^2-(K_{T0}b)^2}, \quad |s| > K_{T0}b \tag{72}$$

$$= -i\sqrt{(K_{T0}b)^2-s^2}, \quad |s| < K_{T0}b$$

Therefore the integral (69) becomes

$$I = -2i\mu_0\alpha^{-1} \int_0^{\infty} s^{-1}\bar{\beta}(s) \sin[s(\eta-\xi)]\, ds. \tag{73}$$

It is evident that as $s \to +\infty$, $s^{-1}\bar{\beta}(s) \to 1$. By considering the relation

$$\int_0^{\infty} \sin[s(\eta-\xi)]\, ds = \frac{1}{\eta-\xi} \tag{74}$$

and setting

$$\bar{P}(\eta,\xi) = \frac{\mu_0}{\pi} \int_0^{\infty} [s^{-1}\bar{\beta}(s)-1] \sin[s(\eta-\xi)]\, ds, \tag{75}$$

eqn (68) becomes

$$\frac{\mu_0}{\pi} \int_{-1}^{1} \frac{\Phi_1(\eta)}{\eta-\xi} d\eta + \int_{-1}^{1} \Phi_1(\eta)\bar{P}(\eta,\xi)\, d\eta = -\tau(\alpha\xi), \quad |\xi| < 1 \tag{76}$$

which is the same form as (C16) of Appendix C for a flat interface crack subjected to SH waves. When $K_{T0}b = O(1)$ or $K_{T0}b \gg 1$ (therefore $K_{T0}r_0 \gg 1$), i.e. the incident wavelength is comparable with or smaller than the debond size and thus very smaller to the inclusion radius, $\tau(\theta)$ on the incident side is identical to that for a SH wave incident on a plane rigid boundary. Therefore, one may say that as $K_{T0}r_0 \gg 1$, a very small debond on the incident side behaves just like a flat interface crack subjected to SH waves. This can be exlained by pointing out that when $K_{T0}r_0 \gg 1$, the curved crack face appears to be a plane to the incident wavelength.

When $K_{T0}b \ll 1$ (therefore $K_{T0}r_0 = O(1)$ or $K_{T0}r_0 \ll 1$), we have the limiting case considered by Yang and Norris (1991). In this case, $\bar{P}(\eta, \xi) \to 0$ and $\tau(\alpha\xi) = \tau(0) + O(\alpha^2)$, thus eqn (76) becomes

$$\frac{\mu_0}{\pi}\int_{-1}^{1}\frac{\Phi_1(\eta)}{\eta-\xi}\mathrm{d}\eta = -\tau(0), \quad |\xi|<1 \tag{77}$$

of which the solution satisfying the single-valued condition (34) is (Muskhelishvili, 1953)

$$\Phi_1(\xi) = -\frac{\tau(0)}{\mu_0}\frac{\xi}{\sqrt{1-\xi^2}} \tag{78}$$

and so

$$\varphi_1(\theta) = -\frac{\tau(0)}{\mu_0}\frac{\theta}{\sqrt{\alpha^2-\theta^2}}. \tag{79}$$

From eqn (22), the COD—Δw—may be expressed, under the substitutions $x = r_0\theta$, as

$$\Delta w(x) = \frac{\tau(0)}{\mu_0}(b^2-x^2)^{1/2} \tag{80}$$

which is the same form as eqn (5.8) of Yang and Norris (1991) if we set $\mu_2 \to \infty$ in their equation.

The DSIF at the tip $\theta = +\alpha$ may be easily derived as

$$K_{\mathrm{III}}^{+} = -\tau(0)\sqrt{b}. \tag{81}$$

The results (80) and (81) are in fact the COD and SSIF of a flat interface crack between a rigid half space and an elastic one subjected to static anti-plane shear loading $\tau(0)$ at infinity and have been obtained by Yang and Norris (1991) for an elastic inclusion. It is not suprising that the debond experiences a quasistatic COD and SIF if we keep in mind that the incident wavelength in this case greatly exceeds the debond size even though $K_{T0}r_0 = O(1)$.

When $K_{T0}r_0 \ll 1$, $\tau(0) \approx 2\tau_0\cos\theta_0$ with $\tau_0 = \mathrm{i}\mu_0 A K_{T0}$. Then eqn (81) becomes

$$K_{\mathrm{III}}^{+} = -2\tau_0\sqrt{b}\cos\theta_0 \tag{82}$$

which can also be obtained from eqn (62) by assuming $\alpha \ll 1$.

The additional RBT due to the small debond is

$$W_1^{(1)} = \frac{\mathrm{i}A\alpha^2}{\pi}h \tag{83}$$

where

$$h = -\frac{\rho H_0^{(1)'}(K_{T0}r_0)}{K_{T0}r_0 H_0^{(1)}(K_{T0}r_0)+2\rho H_0^{(1)'}(K_{T0}r_0)}\cdot\sum_{m=0}^{\infty}\varepsilon_m \mathrm{i}^m \frac{\cos m\theta_0}{H_m^{(1)}(K_{T0}r_0)+2\rho\dfrac{H_0^{(1)'}(K_{T0}r_0)}{K_{T0}r_0}\delta_{0m}} \tag{84}$$

with $\varepsilon_m = 1$ (m = 0) or 2 (m > 0).

The additional scattered far-field pattern is

$$F^{(1)}(\theta,\theta_0) = \frac{\mathrm{i}A\alpha^2}{4\pi^2}g \tag{85}$$

where

$$g = \left\{ \sum_{n=0}^{\infty} \varepsilon_n \mathrm{i}^{-n} \frac{\cos n\theta}{H_n^{(1)}(K_{T0}r_0) + 2\rho \dfrac{H_0^{(1)'}(K_{T0}r_0)}{K_{T0}r_0} \delta_{0n}} \right\} \cdot \left\{ \sum_{m=0}^{\infty} \varepsilon_m \mathrm{i}^{m} \frac{\cos m\theta}{H_m^{(1)}(K_{T0}r_0) + 2\rho \dfrac{H_0^{(1)'}(K_{T0}r_0)}{K_{T0}r_0} \delta_{0m}} \right\}. \quad (86)$$

Equations (83) and (85) show that the presence of a small debond produces changes of order α^2 in the RBT and the far-field displacement. Note please, that eqns (85) and (86) differ from eqns (5.10) and (5.12) of Yang and Norris (1991) in the leading terms of two infinite series. In fact, their result is for a fixed rigid inclusion and may be obtained by setting $\rho \to 0$ in eqn (86).

When $K_{T0}r_0 \ll 1$, g in eqn (86) behaves like

$$g = \pi(K_{T0}r_0)^2 \cos\theta \cos\theta_0 + o[(K_{T0}r_0)^2]. \quad (87)$$

Therefore $F^{(1)}(\theta,\theta_0)$ becomes

$$F^{(1)}(\theta, \theta_0) \approx \frac{A\mathrm{i}}{4}(K_{T0}r_0)^2\alpha^2 \cos\theta \cos\theta_0 \quad (88)$$

which can also be obtained from eqn (67) by assuming $\alpha \ll 1$.

8. NUMERICAL RESULTS AND DISCUSSION

The SCS, DSIF and RBT have been computed for rigid/epoxy combination of inclusion and matrix. The shear modulus and mass density of epoxy may be found in Yang and Norris (1991) and the mass density of the rigid inclusion is taken as $\rho_1 = 2.55$ g mm^{-3} which is the same as that of glass. The computations were checked by (i) comparing the numerical results of the DSIF in the long wavelength limit with the analytical results from eqn (62); (ii) comparing the present results with those of Yang and Norris (1991) and Norris and Yang (1991b) for glass/epoxy combination; (iii) requiring that the optical theorem was satisfied.

In solving eqn (36), we should choose N appropriately to ensure an adequate level of accuracy and to avoid too much CPU time of the computer. To this end, we have computed the DSIF in long wavelength limit by solving eqn (55) numerically with different values of N and compared the results with the analytical solution eqn (62). They are listed in Table 1. It is shown that for a smaller debond $N = 20$–30 may give good accuracy but for a larger debond N should be taken as 40–60. We will choose N based on these results in the following calculations.

Table 1. Comparison between the numerical and analytical results of the DSIF in the long wavelength limit

α (deg)	$-K_{III}/i\tau_0\sqrt{r_0}$ Analytical solution, eqn (62)	$-K_{III}/i\tau_0\sqrt{r_0}$ Numerical solution of eqn (55) $N = 20$	$N = 30$	$N = 40$	$N = 60$
179°	2.3057×10^{-3}	-1.9951×10^{-3}	1.2718×10^{-3}	1.9484×10^{-3}	2.2192×10^{-3}
175°	2.5755×10^{-2}	2.3336×10^{-2}	2.5233×10^{-2}	2.5585×10^{-2}	2.5716×10^{-2}
170°	7.2638×10^{-2}	7.1036×10^{-2}	7.2301×10^{-2}	7.2528×10^{-2}	7.2616×10^{-2}
130°	7.3978×10^{-1}	7.3996×10^{-1}	7.3982×10^{-1}	7.3980×10^{-1}	7.3978×10^{-2}
90°	1.4142	1.4146	1.4143	1.4142	1.4142
60°	1.6119	1.6121	1.6119	1.6119	1.6119
10°	8.3025×10^{-1}	8.3025×10^{-1}	8.3025×10^{-1}	8.3025×10^{-1}	8.3025×10^{-1}
2°	3.7357×10^{-1}	3.7357×10^{-1}	3.7357×10^{-1}	3.7357×10^{-1}	3.7357×10^{-1}

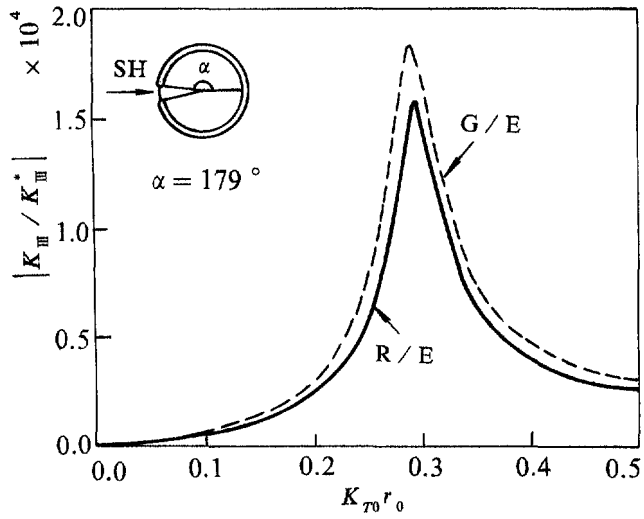

Fig. 2. The absolute-valued DSIF normalized with respect to the static value versus $K_{T0}r_0$ for rigid/epoxy with $\alpha = 179°$ and $\theta_0 = 0°$. The curve for glass/epoxy from Norris and Yang (1991b) is shown for comparison.

The normalized DSIF and SCS for one debond versus $K_{T0}r_0$ in lower frequencies ($K_{T0}r_0 = 0$–1) are depicted in Figs 2 and 3, respectively. The results for glass/epoxy presented by Yang and Norris are also shown for comparison. As we expected, the comparison shows good agreement between the results of the rigid inclusion and those of a glass inclusion because for the glass/epoxy combination $\mu_1/\mu_0 = 23.4 \gg 1$ [see Yang and Norris (1991)], that is, a glass inclusion may be viewed as a rigid one approximately. Indeed, we have indicated before that the analysis and results of Yang and Norris for an elastic inclusion reduce to those for a rigid inclusion with one debond presented in this paper if the shear modulus of the elastic inclusion is infinitely large.

The resonance phenomenon shown in Figs 2 and 3 is called "low frequency resonance" which was discussed in details by Yang and Norris and explicit asymptotic expressions of the response near resonant frequency were derived by Norris and Yang (1991b) for an elastic inclusion with one debond. Their analysis and results can be certainly extended to the case of a rigid inclusion. For instance, eqn (34) in Norris and Yang (1991b), which the

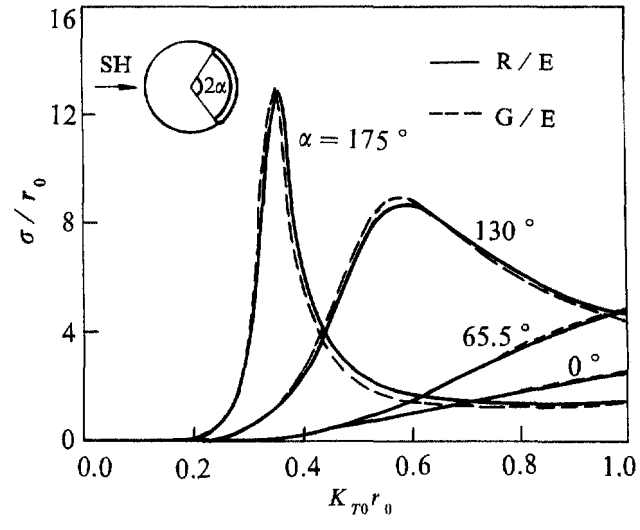

Fig. 3. The SCS versus $K_{T0}r_0$ for rigid/epoxy with $\alpha = 175°$, 130°, 65.5°, 0° and $\theta_0 = 0°$. The curve for glass/epoxy from Yang and Norris (1991) is shown for comparison.

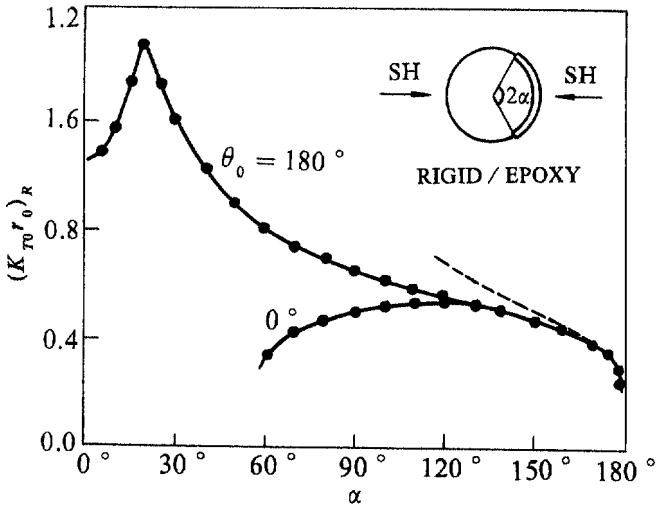

Fig. 4. The resonant frequency of the DSIF versus α for rigid/epoxy with $\theta_0 = 0°$ and 180°. The dashed curve follows from the asymptotic approximation of eqn (89).

resonant frequency satisfies, may be expressed, for a rigid inclusion with a single debond, as

$$\ln\frac{2}{\varepsilon} = \frac{\rho}{(K_{T0}r_0)^2} - \frac{1}{8} + \frac{1}{2}\left[\gamma + \ln\left(\frac{K_{T0}r_0}{2}\right)\right] \tag{89}$$

where $\varepsilon = \pi - \alpha$ (α is the half angular width of the debond), $\rho = \rho_0/\rho_1$ and γ is Euler's constant. The leading-order approximation for $\varepsilon \ll 1$ is

$$K_{T0}r_0 = \sqrt{\rho}\left(\ln\frac{2}{\varepsilon}\right)^{1/2} \tag{90}$$

which shows that the dependence of the resonant frequency upon the debond size α is similar to that for an elastic inclusion. Figures 4–7 illustrate the numerically computed resonant frequencies and resonant peak values of DSIF and SCS as functions of α. The asymptotic results from eqn (89) are also shown in Fig. 4 for comparison. The agreement

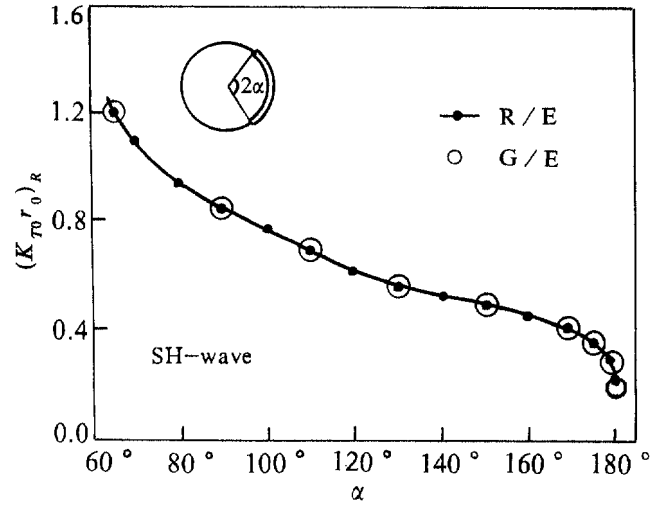

Fig. 5. The resonant frequency of the SCS versus α for rigid/epoxy. The circles are from Yang and Norris (1991) for glass/epoxy.

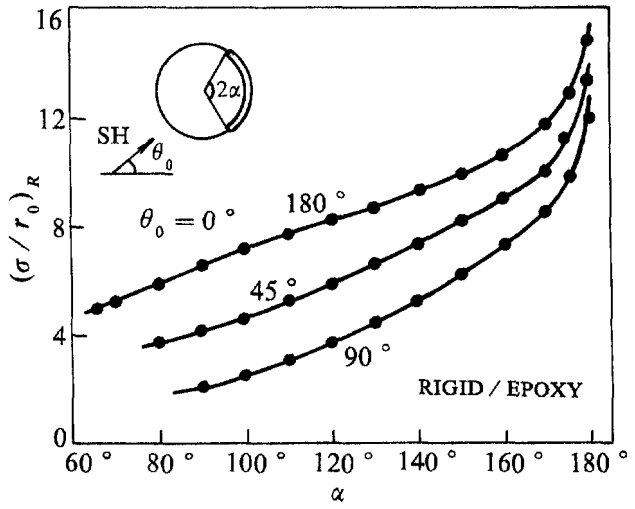

Fig. 6. The resonant peak value of the SCS versus α for rigid/epoxy with $\theta_0 = 0°$, 45°, 90° and 180°.

between the numerical computation and the asymptotic theory is excellent for a large debond ($\alpha > 150°$). The resonances of both DSIF and SCS appear at the same frequency for a larger debond, compare Fig. 4 with Fig. 5, but it is different for a smaller debond. In Fig. 5 the results from Yang and Norris (1991) for glass/epoxy are also presented by circles. These results are in good agreement with those for the rigid inclusion.

The effects of the incident angle θ_0 on the resonance are also shown in Figs 4–7. The resonant frequency of DSIF strongly depends upon θ_0 for a smaller debond ($\alpha < 130°$), but is almost independent of θ_0 for a larger debond ($\alpha \geqslant 130°$). While the incident direction has no influence on the resonant frequency of SCS. The incident wave in 0°—or 180°—direction causes stronger resonance in SCS than those in other directions, see Fig. 6. Furthermore, the detailed computations show that the incident wave in direction θ_0 produces the same SCS as that in direction $(180° - \theta_0)$ does. The influence of θ_0 on the resonant peak value of DSIF is distinct, see Fig. 7 which illustrates the curves for $\theta_0 = 0°$ and 180°. In general, one may say that as the crack tip goes farther into the incident side of the interface, the DSIF becomes higher. This is because: (i) the interface stress on the incident side is higher than that in the shadow side (Pao and Mow, 1973); (ii) the stresses on the crack faces near the tips dominate the DSIFs.

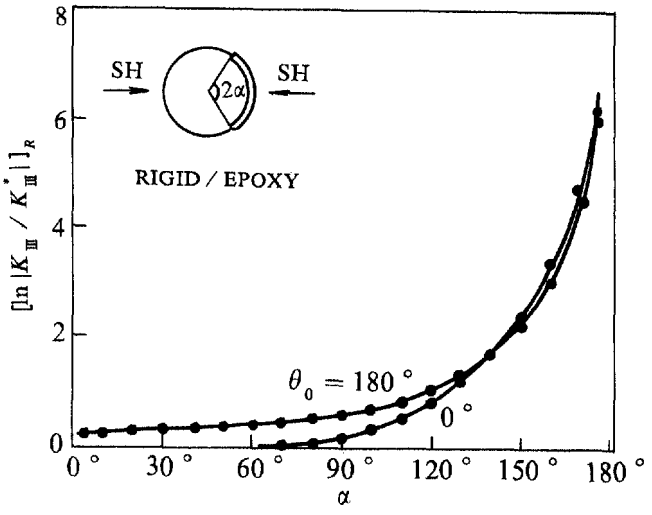

Fig. 7. The logarithmic-valued resonant peak of the normalized DSIF versus α for rigid/epoxy with $\theta_0 = 0°$ and 180°.

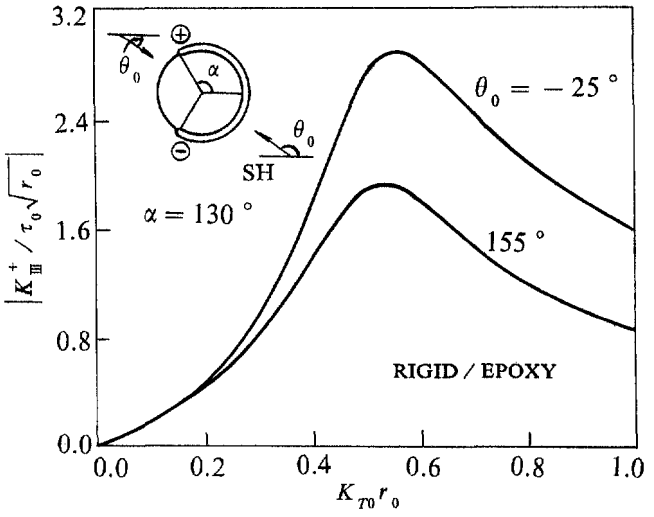

Fig. 8. The absolute-valued DSIF normalized with $\tau_0\sqrt{r_0}$ versus $K_{T0}r_0$ for rigid/epoxy with $\alpha = 130°$ and $\theta_0 = -25°$ and 255°. The relevant static value is zero.

We may note from eqn (62) that the SSIF vanishes when $\theta_0 = (\pi \pm \alpha)/2$ for $0° < \alpha < 180°$. However, the relevant DSIF may reach a high value at a certain frequency, see Fig. 8 which displays a special example for $\alpha = 130°$. Thus, the failure predictions based solely upon static results may break down in situations where the inertial effect is not negligible.

The ratio of the DSIF to the relevant SSIF at higher frequencies is plotted in Fig. 9 for a large debond of $\alpha = 175°$ with $\theta_0 = 0°$ and 180°. The DSIF reduces to small values immediately after reaching a sharp peak at a lower frequency. It is also shown that the values for $\theta_0 = 0°$ remain higher than those for $\theta_0 = 180°$, which we have explained before. Figure 10 illustrates the behavior of the DSIF at higher frequencies for a small debond of $\alpha = 2°$. The approximate results in the small debond limit given by eqn (81) for $\theta_0 = 180°$ are shown by a dashed curve. Although eqn (81) is derived under the assumption of $K_{T0}r_0 = O(1)$, the numerical calculations show that it is valid even when $K_{T0}r_0 = 6$. The dotted curve shown in Fig. 10 is the result for a flat interface crack subjected to SH waves given in Appendix C. It agrees well with that for a small debond at higher frequencies ($K_{T0}r_0 > 6$). It should be noted that the DSIF for $\theta_0 = 0°$ reduces rapidly to very small values at higher frequencies, that is, a small debond in the shadow side does not exhibit a

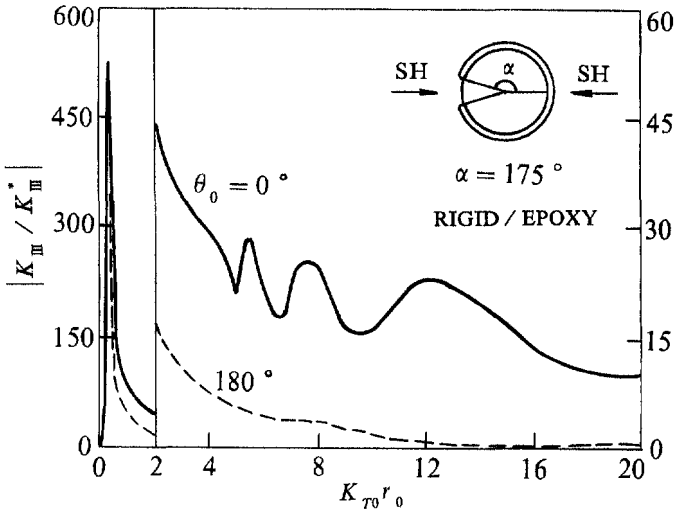

Fig. 9. The absolute-valued normalized DSIF at high frequencies for rigid/epoxy with $\alpha = 175°$ and $\theta_0 = 0°$ and 180°.

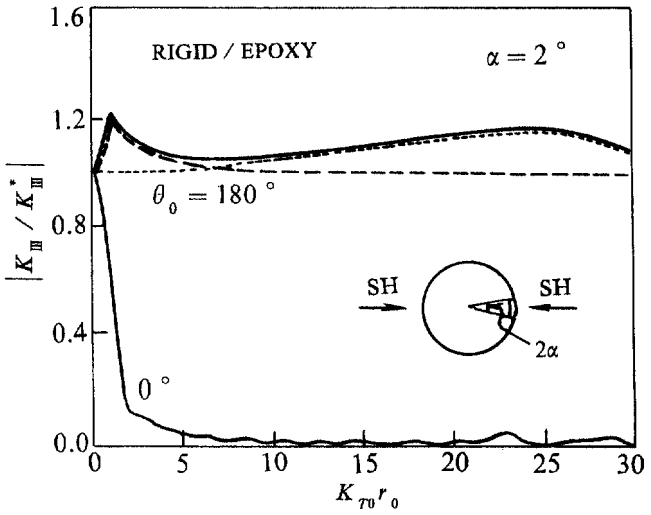

Fig. 10. The absolute-valued normalized DSIF for rigid/epoxy with a small debond ($\alpha = 2°$) and $\theta_0 = 0°, 180°$. The dotted curve is from Appendix C for a flat interface crack and the dashed curve is from the asymptotic approximation of eqn (81) for the small debond limit.

dynamic behavior like a flat interface crack at higher frequencies. In conclusion, the numerical results shown in Fig. 10 for a small debond support the analysis presented in Section 7.

The normalized RBT for one debond versus $K_{T0}r_0$ is shown in Fig. 11, which also demonstrates a low frequency resonance phenomenon like the SCS.

The influence of the mass density ratio ρ_1/ρ_0 on the SCS and DSIF is displayed in Figs 12 and 13 for $\alpha = 175°$ and $\theta_0 = 0°$. As ρ_1/ρ_0 is increased, the resonance becomes more pronounced and occurs at lower frequency, which could be seen clearly from the asymptotic expression given by eqns (89) or (90). The asymptotic solution from eqn (89) for the resonant frequency of the DSIF is compared with the numerical solution in Fig. 14 which shows good agreement between these two solutions. In the limiting case where $\rho_1/\rho_0 \to \infty$, i.e. the inclusion is fixed, the DSIF and SCS become infinitely large as $K_{T0}r_0 \to 0$, which means that the resonant frequency approaches to zero. What this implies is that if the inclusion were to be fixed stationary in space, it would have to exert infinite force on the medium in order to be in static equilibrium. This is what one would expect physically.

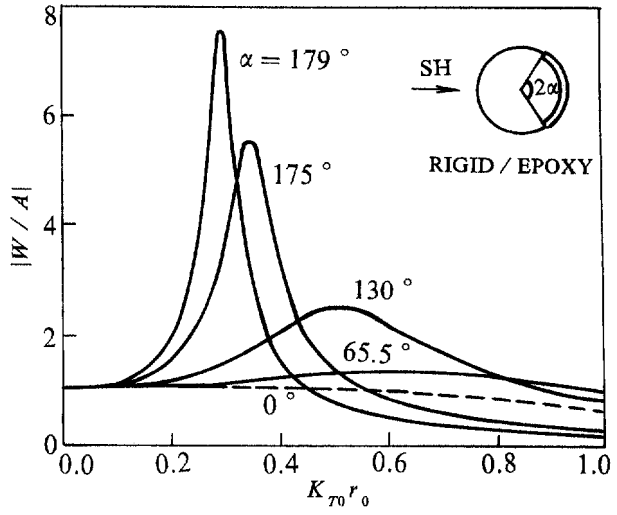

Fig. 11. The absolute-valued RBT versus $K_{T0}r_0$ for rigid/epoxy with $\alpha = 179°, 175°, 130°, 65.5°, 0°$ (dashed curve) and $\theta_0 = 0°$.

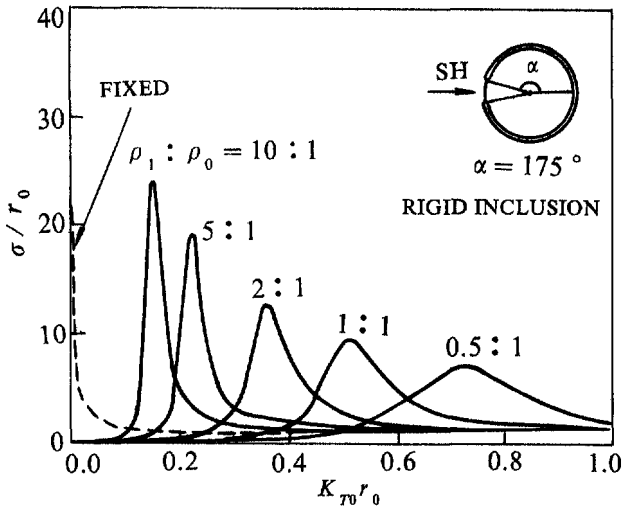

Fig. 12. The SCS versus $K_{T0}r_0$ for different values of ρ_1/ρ_0 with $\alpha = 175°$ and $\theta_0 = 0°$. The dashed curve is for a fixed rigid inclusion (i.e. $\rho_1/\rho_0 = \infty$).

The SCS for two debonds of the same size $\alpha = 65°$ is illustrated in Fig. 15 versus $K_{T0}r_0$. A distinct resonance also appears at a lower frequency in this case and it depends upon the relative positions of the debonds evidently. As two debonds are closer to each other (i.e. β in the figure is decreased) the resonance becomes more pronounced and will very slowly approach the corresponding case of one debond as $\beta \to 0°$, compare the curves in Fig. 15 with that of $\alpha = 130°$ in Fig. 3.

The DSIF normalized with relevant SSIF for two debonds of the same size $\alpha = 85°$ is illustrated in Fig. 16 as a function of $K_{T0}r_0$. Although the angular width of each bonding region is only 10°, the resonance is not so strong as that shown in Fig. 9 for one debond.

In conclusion, the scattering problem of SH waves from a rigid inclusion with multiple debonds along the interface is solved by using a method different from those of Yang and Norris (1991) and Norris and Yang (1991b). The numerical results and the analytical solutions in two limiting cases—the long wavelength limit and the small debond limit are in good agreement with those of Yang and Norris. Therefore the method is proved to be

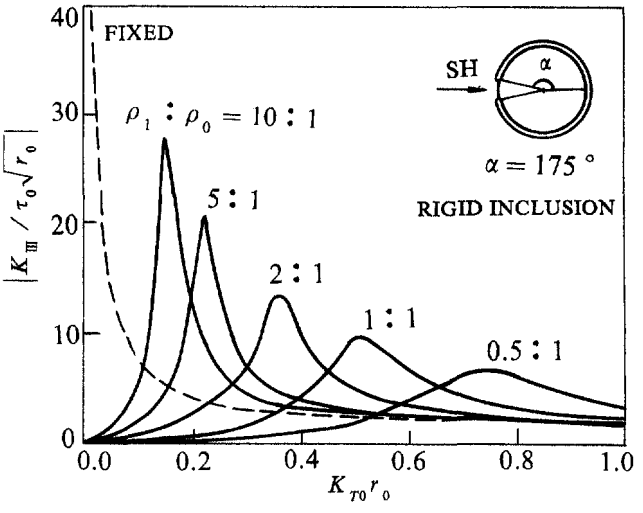

Fig. 13. The absolute-valued DSIF normalized with $\tau_0\sqrt{r_0}$ versus $K_{T0}r_0$ for different values of ρ_1/ρ_0 with $\alpha = 175°$ and $\theta_0 = 0°$. The dashed curve is for a fixed rigid inclusion (i.e. $\rho_1/\rho_0 = \infty$).

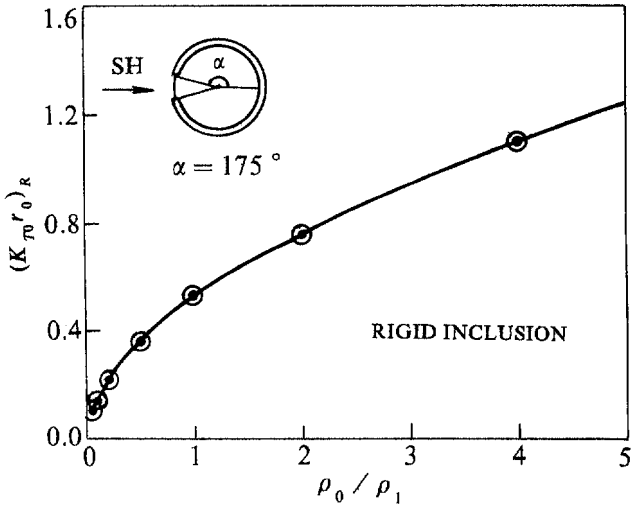

Fig. 14. The resonant frequency of the DSIF versus ρ_0/ρ_1 for $\alpha = 175°$ and $\theta_0 = 0°$. The curve is from the asymptotic approximation of eqn (89).

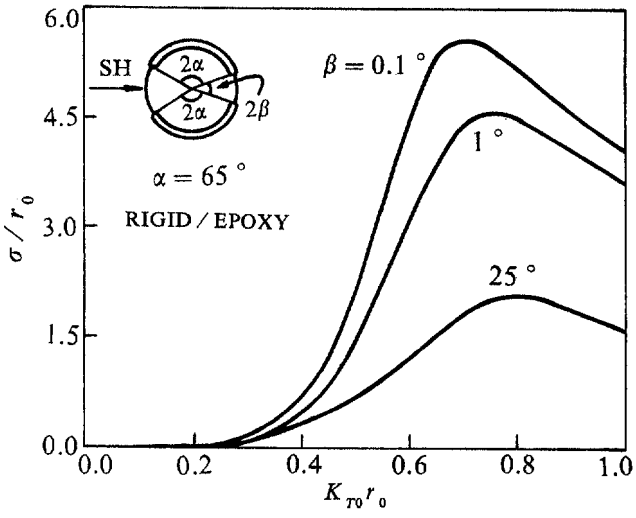

Fig. 15. The SCS versus $K_{T0}r_0$ for rigid/epoxy with two debonds of the same size. The effect of their relevant position (the angle β) is shown.

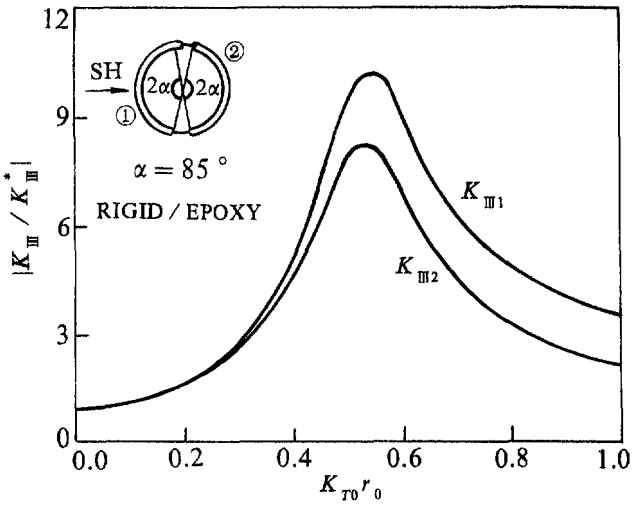

Fig. 16. The absolute-valued normalized DSIF versus $K_{T0}r_0$ for rigid/epoxy with two debonds of the same size.

successful. One advantage of the present method is that it can be easily applied to the in-plane problem involving the oscillatory singular behavior of the stresses near the crack tips which we will deal with in Part II of this two-part paper.

REFERENCES

Abromowitz, M. and Stegun, I. A. (1965). *Handbook of Mathematical Functions*. Dover, New York.

Belyaev, K. P. (1985). Interaction of a shear wave with an elastic cylindrical inclusion having a crack along its contour. *Prikl. Mekh.* **21** (9), 112–116.

Boström, A. (1987). Elastic wave scattering from an interface crack: Antiplane strain. *J. Appl. Mech.* **54,** 503–508.

Boström, A. and Olsson, P. (1987). Scattering of elastic waves by non-planar cracks. *Wave Motion* **9,** 61–76.

Coussy, O. (1982). Scattering of SH-waves by a cylindrical inclusion presenting an interfacial crack. *C. R. Acad. Sci. Paris* **295,** 1043–1046.

Coussy, O. (1983). Scattering of elastic waves by an inclusion with an interface crack. *Wave Motion* **6,** 223–236.

Erdogan, F. and Gupta, G. D. (1971). Layered composites with a interface flaw. *Int. J. Solids Structures* **7,** 1089–1107.

Erdogan, F. and Gupta, G. D. (1972). On the numerical solution of singular integral equations. *Q. Appl. Math.* **29,** 525–534.

Kitahara, M., Nakagawa, K. and Achenbach, J. D. (1989). Backscatter from a spherical inclusion with compliant interphase characteristics. In *Review of Progress in QNED*, Vol. 8A (Edited by D. O. Thompson and D. E. Chimenti), pp. 47–54. Plenum, New York.

Lu, Ch. K. (1965). On singular integral equation with Hilbert kernel (in Chinese). *Adv. Math.* (Chinese edition) **8,** 161–167.

Miklowitz, J. (1978). *The Theory of Elastic Waves and Wave Guides*. North Holland, Amsterdam.

Muskhelishvili, N. I. (1953). *Singular Integral Equations*. Noordhoff, Leyden.

Norris, A. N. and Yang, Y. (1991a). Static and dynamic axial loading of a partially bonded fiber. *Mech. Mater.* **11,** 163–175.

Norris, A. and Yang, Y. (1991b). Dynamic stress on a partially bonded fiber. *J. Appl. Mech.* **58,** 404–409.

Olsson, P. and Boström, A. (1989). Dynamic stress intensity factors for 3D non-planar cracks. In *Elastic Wave Propagation* (Edited by M. F. McCarthy and M. A. Hayes), pp. 399–404. North Holland, Amsterdam.

Pao, Y. H. and Mow, C. C. (1973). *Diffraction of Elastic Waves and Dynamic Stress Concentrations*. Crane and Russak, New York.

Parton, V. Z. and Kudryavtsev, B. A. (1975). Dynamic problem of fracture mechanics for a plane with an inclusion. In *Mechanics of Deformable Bodies and Constructions* (in Russian), pp. 379–384. Mashinostroyenige, Moscow.

Yang, H. J. and Bogy, B. B. (1985). Elastic wave scattering from an interface carck in a layered half-space. *J. Appl. Mech.* **52,** 42–50.

Yang, Y. and Norris, A. N. (1991). Shear wave scattering from a debonded fiber. *J. Mech. Phys. Solids* **39,** 273–294.

Yang, Y. and Norris, A. (1992). Longitudinal wave scattering from a partially bonded fiber. *Wave Motion* **15,** 43–59.

Zhong, W. and Lin, Q. (1992). A boundary element method to scattering of elastic wave for anisotropic medium (in Chinese). *Acta Mech. Solida Sin.* (Chinese edition) **14,** 214–244.

APPENDIX A: EVALUATION OF INTEGRAL IN EQN (61)

We evaluate the integral

$$I = \int_{-\alpha}^{\alpha} \cos(\zeta - \theta_0) \sqrt{\frac{\tan\frac{\alpha}{2} + \tan\frac{\zeta}{2}}{\tan\frac{\alpha}{2} - \tan\frac{\zeta}{2}}}\, d\zeta. \tag{A1}$$

Making the change of variable: $u = \tan\frac{\zeta}{2}/\tan\frac{\alpha}{2}$, we may express eqn (A1) as

$$I = 4\tan\frac{\alpha}{2}\left[I_1 \cos\theta_0 + I_2 \tan\frac{\alpha}{2}\sin\theta_0\right] \tag{A2}$$

where

$$I_1 = \int_0^1 \frac{1 - u^2\tan^2\frac{\alpha}{2}}{\left(1 + u^2\tan^2\frac{\alpha}{2}\right)^2} \frac{du}{\sqrt{1-u^2}}, \quad I_2 = \int_0^1 \frac{2u^2}{\left(1 + u^2\tan^2\frac{\alpha}{2}\right)^2} \frac{du}{\sqrt{1-u^2}}. \tag{A3}$$

We first evaluate I_2. Set $u = \sin\eta$, then

$$I_2 = 2\int_0^{\frac{\pi}{2}} \frac{\sin^2\eta}{\left(1 + \sin^2\eta\tan^2\frac{\alpha}{2}\right)^2} d\eta \tag{A4}$$

which can be further expressed, under the substitution $t = \tan\eta$, as

$$I_2 = 2\int_0^{\infty} \frac{t^2}{\left(1 + t^2\sec^2\frac{\alpha}{2}\right)^2} dt = 2\cos^2\frac{\alpha}{2}\left[\int_0^{\infty} \frac{dt}{1 + t^2\sec^2\frac{\alpha}{2}} - \int_0^{\infty} \frac{dt}{\left(1 + t^2\sec^2\frac{\alpha}{2}\right)^2}\right]. \tag{A5}$$

Considering that

$$\int \frac{dt}{1 + t^2\sec^2\frac{\alpha}{2}} = \cos\frac{\alpha}{2}\tan^{-1}\left(t\sec\frac{\alpha}{2}\right) \tag{A6}$$

$$\int \frac{dt}{\left(1 + t^2\sec^2\frac{\alpha}{2}\right)^n} = \frac{t}{2(n-1)\left(1 + t^2\sec^2\frac{\alpha}{2}\right)^{n-1}} + \frac{(2n-3)}{2(n-1)}\int \frac{dt}{\left(1 + t^2\sec^2\frac{\alpha}{2}\right)^{n-1}}, \tag{A7}$$

we obtain

$$I_2 = \frac{\pi}{2}\cos^3\frac{\alpha}{2}. \tag{A8}$$

The integral I_1 may be expressed as

$$I_1 = \int_0^1 \frac{1}{1 + u^2\tan^2\frac{\alpha}{2}} \frac{du}{\sqrt{1-u^2}} - I_2\tan^2\frac{\alpha}{2} \tag{A9}$$

where the first integral, by making the change of variables from u to t as before, may be evaluated as

$$\int_0^1 \frac{1}{1 + u^2\tan^2\frac{\alpha}{2}} \frac{du}{\sqrt{1-u^2}} = \int_0^{\infty} \frac{dt}{1 + t^2\sec^2\frac{\alpha}{2}} = \frac{\pi}{2}\cos\frac{\alpha}{2}. \tag{A10}$$

Therefore

$$I_1 = \frac{\pi}{2}\cos^3\frac{\alpha}{2}. \tag{A11}$$

APPENDIX B: EVALUATION OF THE DOUBLE INTEGRAL IN EQN (66)

We evaluate the double integral

$$\mathrm{II} = \int_{-\alpha}^{\alpha} X(\eta)\sin(\eta-\theta)\int_{-\alpha}^{\alpha}\cos(\zeta-\theta_0)X^{-1}(\zeta)\left[\cot\left(\frac{\zeta-\eta}{2}\right)-\tan\frac{\eta}{2}\right]\mathrm{d}\zeta\,\mathrm{d}\eta \tag{B1}$$

where $X(\eta)$ is given by (59).

By considering the odevity of the integrand, eqn (B1) becomes

$$\mathrm{II} = \mathrm{II}_1\cos\theta\cos\theta_0 + \mathrm{II}_2\sin\theta\sin\theta_0 \tag{B2}$$

where

$$\mathrm{II}_1 = \int_{-\alpha}^{\alpha}\frac{\sin\eta}{\sqrt{\tan^2\frac{\alpha}{2}-\tan^2\frac{\eta}{2}}}\int_{-\alpha}^{\alpha}\cos\zeta\sqrt{\tan^2\frac{\alpha}{2}-\tan^2\frac{\zeta}{2}}\frac{\sec^2\frac{\eta}{2}}{\tan\frac{\zeta}{2}-\tan\frac{\eta}{2}}\mathrm{d}\zeta\,\mathrm{d}\eta \tag{B3}$$

$$\mathrm{II}_2 = \int_{-\alpha}^{\alpha}\frac{\cos\eta}{\sqrt{\tan^2\frac{\alpha}{2}-\tan^2\frac{\eta}{2}}}\int_{-\alpha}^{\alpha}\sin\zeta\sqrt{\tan^2\frac{\alpha}{2}-\tan^2\frac{\zeta}{2}}\frac{\sec^2\frac{\eta}{2}}{\tan\frac{\zeta}{2}-\tan\frac{\eta}{2}}\mathrm{d}\zeta\,\mathrm{d}\eta. \tag{B4}$$

We first evaluate II_1. By making an exchange of the integral order, II_1 can be rewritten as

$$\mathrm{II}_1 = \int_{-\alpha}^{\alpha}\cos\zeta\sqrt{\tan^2\frac{\alpha}{2}-\tan^2\frac{\zeta}{2}}\,\bar{\mathrm{I}}_1(\zeta)\,\mathrm{d}\zeta \tag{B5}$$

where

$$\bar{\mathrm{I}}_1(\zeta) = \int_{-\alpha}^{\alpha}\frac{\sin\eta}{\sqrt{\tan^2\frac{\alpha}{2}-\tan^2\frac{\eta}{2}}}\frac{\sec^2\frac{\eta}{2}}{\tan\frac{\zeta}{2}-\tan\frac{\eta}{2}}\mathrm{d}\eta. \tag{B6}$$

Make the change of variables from η to t as we have done in Appendix A. Then eqn (B6) becomes

$$\bar{\mathrm{I}}_1(\zeta) = 4\tan\frac{\alpha}{2}\int_0^{\infty}\left[\frac{-2\cos^2\frac{\zeta}{2}}{1+t^2\sec^2\frac{\alpha}{2}}+\frac{2\sin^2\frac{\zeta}{2}}{\tan^2\frac{\zeta}{2}+t^2\left(\tan^2\frac{\zeta}{2}-\tan^2\frac{\alpha}{2}\right)}\right]\mathrm{d}t \tag{B7}$$

which can be evaluated, by using eqn (A6), as

$$\bar{\mathrm{I}}_1(\zeta) = -4\pi\sin\frac{\alpha}{2}\cos^2\frac{\zeta}{2}+2\pi\tan\frac{\alpha}{2}\sin\zeta\left(\tan^2\frac{\zeta}{2}-\tan^2\frac{\alpha}{2}\right)^{-1/2}. \tag{B8}$$

Therefore

$$\mathrm{II}_2 = -4\pi\sin\frac{\alpha}{2}\int_{-\alpha}^{\alpha}\cos^2\frac{\zeta}{2}\cos\zeta\sqrt{\tan^2\frac{\alpha}{2}-\tan^2\frac{\zeta}{2}}\,\mathrm{d}\zeta-2i\pi\tan\frac{\alpha}{2}\int_{-\alpha}^{\alpha}\cos\zeta\sin\zeta\,\mathrm{d}\zeta. \tag{B9}$$

The second integral in eqn (B9) is equal to zero and the first one, by making the change of variables from ζ to t as before, may be expressed as

$$\int_{-\alpha}^{\alpha}\cos^2\frac{\zeta}{2}\cos\zeta\sqrt{\tan^2\frac{\alpha}{2}-\tan^2\frac{\zeta}{2}}\,\mathrm{d}\zeta=4\tan\frac{\alpha}{2}\int_0^{\infty}\frac{1+t^2\left(1-\tan^2\frac{\alpha}{2}\right)}{\left(1+t^2\sec^2\frac{\alpha}{2}\right)^3}\,\mathrm{d}t$$

$$=4\tan\frac{\alpha}{2}\left\{\int_0^{\infty}\frac{\mathrm{d}t}{\left(1+t^2\sec^2\frac{\alpha}{2}\right)^2}-2\sin^2\frac{\alpha}{2}\left[\int_0^{\infty}\frac{\mathrm{d}t}{\left(1+t^2\sec^2\frac{\alpha}{2}\right)^2}-\int_0^{\infty}\frac{\mathrm{d}t}{\left(1+t^2\sec^2\frac{\alpha}{2}\right)^3}\right]\right\}. \tag{B10}$$

Making use of eqns (A6) and (A7), we have

$$\mathrm{II}_1=-2\pi^2\left(1-\cos^4\frac{\alpha}{2}\right). \tag{B11}$$

Integral II_2 may also be evaluated similarly. We omit the detailed analysis and only give the final result which is

$$\mathrm{II}_2=-2\pi^2\sin^4\frac{\alpha}{2}. \tag{B12}$$

APPENDIX C: SCATTERING OF SH WAVES BY A FLAT INTERFACE CRACK

The scattering of SH waves by a flat interface crack between two elastic half spaces has been studied by Boström (1987). He obtained an integral equation in terms of the COD and presented the numerical results for the far-field amplitude and scattered energy. Here, we consider an interface crack between a rigid half space and an elastic one by a different method. A Cauchy singular integral equation is derived with the dislocation density function as the unknown and a formula for calculating the DSIF is given.

Consider the problem shown in Fig. C1. A flat crack with length $2b$ lies on the interface between a rigid half space and an elastic one. An incident SH wave propagates in the θ_0 direction. Take Cartesian coordinates (x, y) as shown, with the origin at the centre of the crack. All motion is time harmonic with frequency ω, and the term $\mathrm{e}^{-i\omega t}$ will be omitted. Decomposed the total out-of-plane displacement in the elastic half space as

$$w_0(x,y)=w_0^{(i)}(x,y)+w_0^{(r)}(x,y)+w_0^{(s)}(x,y) \tag{C1}$$

where $w_0^{(i)}$ represents the incident wave with the form of eqn (1) which may be rewritten as

$$w_0^{(i)}(x,y)=A\,\mathrm{e}^{iK_{T0}(x\cos\theta_0-y\sin\theta_0)}, \tag{C2}$$

$w_0^{(r)}$ represents the reflected wave from a plane rigid boundary which is (Miklowitz, 1987)

$$w_0^{(r)}(x,y)=-A\,\mathrm{e}^{iK_{T0}(x\cos\theta_0-y\sin\theta_0)}, \tag{C3}$$

and $w_0^{(s)}$ is the scattered field by the interface crack, which satisfies the Helmholtz equation

$$\nabla^2 w_0^{(s)}+K_{T0}^2 w_0^{(s)}=0,\quad y<0 \tag{C4}$$

with $\nabla^2=(\partial^2/\partial x^2)+(\partial^2/\partial y^2)$. The solution of eqn (C4) in the form of Fourier representation is

$$w_0^{(s)}=\int_{-\infty}^{\infty}f(s)\,\mathrm{e}^{i\alpha x+\beta y}\,\mathrm{d}s \tag{C5}$$

where

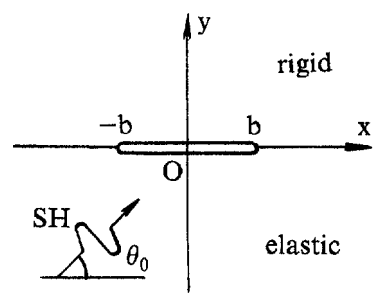

Fig. C1. A flat interface crack between a rigid half space and an elastic one subjected to an incident SH wave.

$$\beta = \sqrt{s^2 - K_{T0}^2}, \quad |s| > K_{T0} \tag{C6}$$
$$= -\mathrm{i}\sqrt{K_{T0}^2 - s^2}, \quad |s| < K_{T0}.$$

On the interface, $w_0^{(s)} = 0$ for $|x| > b$ or $w_0^{(s)} = -\Delta w(x)$ (the COD of the crack) for $|x| < b$. This gives

$$\int_{-\infty}^{\infty} f(s)\, \mathrm{e}^{\mathrm{i}sx}\, \mathrm{d}s = \begin{cases} 0, & |x| > b \\ -\Delta w(x), & |x| < b. \end{cases} \tag{C7}$$

Inverting the Fourier transform in eqn (C7), we have

$$f(s) = \frac{1}{2\pi}\int_{-b}^{b} \Delta w(u)\, \mathrm{e}^{-\mathrm{i}su}\, \mathrm{d}u. \tag{C8}$$

Along the cracked part of the interface the traction vanishes and thus

$$\mu_0\left(\frac{\partial w^{(i)}}{\partial y} + \frac{\partial w^{(r)}}{\partial y} + \frac{\partial w^{(s)}}{\partial y}\right) = 0, \quad y = 0, \quad |x| < b \tag{C9}$$

which gives with eqns (C5) and (C8)

$$-\frac{\mu_0}{2\pi}\int_{-\infty}^{\infty} \beta\, \mathrm{e}^{\mathrm{i}sx} \int_{-b}^{b} \Delta w(u)\, \mathrm{e}^{-\mathrm{i}su}\, \mathrm{d}u\, \mathrm{d}s = -\tau(x), \quad |x| < b \tag{C10}$$

where

$$\tau(x) = \mu_0\left(\frac{\partial w^{(i)}}{\partial y} + \frac{\partial w^{(r)}}{\partial y}\right)_{y=0}.$$

Equation (C10) is the integral equations for the COD which coincides with eqn (15) of Boström (1987) if we set $\mu_1 \to \infty$ in his equation. We further introduce a dislocation density function

$$\varphi(x) = \frac{\partial}{\partial x}(\Delta w) \tag{C11}$$

which means

$$\Delta w(x) = \int_{-b}^{x} \varphi(u)\, \mathrm{d}u. \tag{C12}$$

Obviously, $\int_{-b}^{b} \varphi(x)\, \mathrm{d}x = 0$. Substituting eqn (C12) into eqn (C10) and using the by-part interation yield

$$\frac{\mathrm{i}\mu_0}{2\pi}\int_{-b}^{b} \varphi(u)\left[\int_{-\infty}^{\infty} s^{-1}\beta\, \mathrm{e}^{\mathrm{i}s(x-u)}\, \mathrm{d}s\right]\mathrm{d}u = -\tau(x), \quad |x| < b. \tag{C13}$$

If we set

$$P(u,x) = \frac{\mathrm{i}\mu_0}{2\pi}\int_{-\infty}^{\infty} [s^{-1}\beta - \mathrm{sgn}(s)]\, \mathrm{e}^{\mathrm{i}s(x-u)}\, \mathrm{d}s = \frac{\mu_0}{\pi}\int_0^{\infty} (s^{-1}\beta - 1)\sin[s(u-x)]\, \mathrm{d}s \tag{C14}$$

and use the relation (74), eqn (C13) becomes

$$\frac{\mu_0}{\pi}\int_{-b}^{b} \frac{\varphi(u)}{u-x}\mathrm{d}u + \int_{-b}^{b} \varphi(u)P(u,x)\, \mathrm{d}u = -\tau(x), \quad |x| < b \tag{C15}$$

which, by using the substitutions $u = b\eta$, $x = b\xi$ and $\Phi(\eta) = \varphi(b\eta)$, can be rewritten as

$$\frac{\mu_0}{\pi}\int_{-1}^{1} \frac{\Phi(\eta)}{\eta - \xi}\mathrm{d}\eta + \int_{-1}^{1} \Phi(\eta)\bar{P}(\eta,\xi)\, \mathrm{d}\eta = -\tau(b\zeta), \quad |\xi| < 1 \tag{C16}$$

where

$$\bar{P}(\eta,\xi) = \frac{\mu_0}{\pi}\int_0^{\infty} [t^{-1}\bar{\beta}(t) - 1]\sin[t(\eta - \zeta)]\, \mathrm{d}t \tag{C17}$$

with $\bar{\beta} = \sqrt{t^2 - (K_{T0}b)^2}$ for $|t| > K_{T0}b$ or $-\mathrm{i}\sqrt{(K_{T0}b)^2 - t^2}$ for $|t| < K_{T0}b$.

In addition, $\Phi(\xi)$ should also satisfy the single-valued condition

$$\int_{-1}^{1} \Phi(\xi)\, d\xi = 0. \tag{C18}$$

Equation (C16) is a standard Cauchy singular integral equation of the first kind and can be solved numerically by the method we outlined in Section 3. The DSIFs are defined as

$$K_{III\pm} = \lim_{x \to \pm b^{\pm}} [\sqrt{2(\pm x - b)}\tau_{yz}(x)] \tag{C19}$$

where $\tau_{yz}(x)$ is the shear stress along the interface beyond the crack. By following the analysis similar to that in Section 4, it can be easily derived that

$$K_{III\pm} = \mu_0 \sqrt{b} F(\pm 1) \tag{C20}$$

where $F(\xi) = \Phi(\xi)\sqrt{1-\xi^2}$. The corresponding SSIFs are

$$K^*_{III\pm} = -2\tau_0 \sin\theta_0 \sqrt{b} \tag{C21}$$

with $\tau_0 = i\mu_0 A K_{T0}$.